Optimal contact sensor mounting position for impulsive excitation technique

Abdul Rahim Bahari [1], Mohd Zaki Nuawi [2], Ahmad Azlan Mat Isa [1], Mahfodzah Md Padzi [3], Zairi Ismael Rizman [4, *]

[1]Faculty of Mechanical Engineering, Terengganu Branch, Bukit Besi Campus, 23200 Dungun, Terengganu, Malaysia
[2]Faculty of Engineering and Built Environment, Universiti Kebangsaan Malaysia, 43600 Bangi, Selangor, Malaysia
[3]Mechanical Section, Malaysia France Institute, Universiti Kuala Lumpur, Section 14, 43650 Bandar Baru Bangi, Selangor, Malaysia
[4]Faculty of Electrical Engineering, Universiti Teknologi MARA, Terengganu Branch, Dungun Campus, 23000 Dungun, Terengganu, Malaysia

A B S T R A C T

Impulsive excitation is a non-destructive test to determine the elastic properties of materials. The transient-decaying signal can be measured using a contact or non-contact type of sensor. The aim of this study is to assess the optimal contact sensor position for an impulsive excitation test purpose. Rectangular bar of medium carbon steel S50C is considered as a specimen in the experimental test with various contact sensor positions. The vibration dynamic responses in the resonant frequency in flexure mode from various different contact sensor positions are statistically analyzed to measure the precision of each position and to determine the significance differences among the all the positions.

1. Introduction

Material characterization describes features of the composition and structure including defects of a material that are significant for a particular preparation, study of properties and suffice for the reproduction of the material (Groves and Wachtman, 1985). A knowledge of material properties is fundamental for the complete characterization of engineering materials (Alfano and Pagnotta, 2007) and very important for mechanical design, research and engineering applications. The material properties determine the range of usefulness of the material and establish the service that can be expected. For elastic properties of a material, it can be determined using destructive or non-destructive method. Non-destructive method refers to the impulsive excitation technique, which is also known as a dynamic mechanical test. It consists of setting a sample into mechanical vibration in one or more vibrational mode at one or more frequencies at which the vibrational displacements are at a maximum. The elastic properties can be determined from the vibrational modes and natural frequencies

of the vibration decay, mass and dimension of the sample (Botelho et al., 2006; Radovic et al., 2004). To set the specimen into the vibrational mode needs an impulser such as a loudspeaker, a modal hammer (Sanliturk and Koruk, 2013; Plachy et al., 2009), a small steel ball attached to an elastic rod (Raggio et al., 2007; Salem and Singh, 2006), free falling release of a small ball from a certain height to the specimen (Tognana et al., 2010; Ito and Uomoto, 1997), a steel sphere driven by a linear solenoid actuator (Liu et al., 2011) and a shaker (Renault et al., 2011).

The impulsive excitation technique has been applied in various science and technology disciplines. Alfano and Pagnotta (2007) applied a non-destructive technique for determining the dynamic elastic properties of isotropic thin square plates. Botelho et al. (2006) obtained the viscoelastic properties such as elastic and viscous responses for aluminum 2024 alloy, carbon fiber/epoxy, glass fiber/epoxy and their hybrid aluminum 2024 alloy/carbon fiber/epoxy and aluminum 2024 alloy/glass fiber/epoxy composites. Ito and Uomoto (1997) evaluated the degradation of stiffness of concrete due to crack progress by the impulsive excitation method. Liu et al. (2011) developed a rapid and effective non-destructive testing and evaluation technique in order to assess the tile-wall bonding quality to prevent the danger caused by falling tiles from high-rise buildings. The impulsive excitation technique has several advantages such as

high precision result, lower cost and repeatability because of simple equipment, ease of specimen preparation, wide variety of specimen shapes and sizes, and also can be repeated for another test measurement over a wide temperature range. A sensor is an object whose purposes are to detect events or changes in its environment and then provide a corresponding output. It is an input device that provides a usable output in response to a specific physical quantity input (Nyce, 2004). A sensor (Abidin et al., 2017) is a type of transducer and may provide various types of output, but typically use electrical or optical signals. The vibrational behavior of the samples can be represented by various types of signals such as vibration, sound or acoustic, strain and piezo signals. This sensor can be categorized to a contact sensor and non-contact sensor. Contact type needs to mount the sensor at the surface of the specimen. Some researches that applied contact sensor method are accelerometer (Policarpo et al., 2013; Prasad and Seshu, 2008) and piezoelectric transducer. Non-contact sensor is used by placing the sensor closely to the specimen. An example of the non-contact sensor is a microphone (Santos et al., 2013; Tong et al., 2006).

Fundamental resonant frequency of sample is required to determine the dynamic Young's modulus of the material using (Eq. 1)

$$E = 0.9465(\frac{mf_f^2}{b})(\frac{L^3}{t^3})T_1 \qquad (1)$$

where E is Young's modulus, m is mass of the sample, b is width of the sample, L is length of the specimen, t is thickness of the sample, f_f is fundamental resonant frequency of sample in flexure and T1 is correction factor for fundamental flexural mode to account for finite thickness of sample, Poisson's ratio and so forth. Equation for T_1 is as follow (Eq. 2)

$$T_1 = 1 + 6.585(1 + 0.0752\mu + 0.8109\mu^2)(t/L)^2 - 0.868\left(\frac{t}{L}\right)^4 - \left[\frac{8.340(1+0.2023\mu+2.173\mu^2)(t/L)^4}{1.000+6.338(1+0.1408\mu+1.536\mu^2(t/L)^2}\right] \qquad (2)$$

where μ is Poisson's ratio.

The algorithm used to obtain the fundamental resonant frequency and to transform samples of the data from the time domain into the frequency domain is the Discrete Fourier Transform (DFT). The DFT establishes the relationship between the samples of a signal in the time domain and their representation in the frequency domain. The DFT is widely used in the fields of spectral analysis, applied mechanics, acoustics, medical imaging, numerical

analysis, instrumentation and telecommunications. DFT is given by (Eq. 3)

$$X_N(k) = \sum_{n=0}^{N-1} x(n)e^{-j2\pi kn/N} \qquad (3)$$

Inverse Discrete Fourier Transform (IDFT) is defined as (Eq. 4)

$$x_n = \frac{1}{N}\sum_{k=0}^{N-1} X_N(k)e^{j2\pi kn/N} \qquad (4)$$

where $X_N(k)$ is an N point DFT of x_n. Note that $X_N(k)$ is a function of a discrete integer k, where k ranges from 0 to N-1.

The Fast Fourier Transform (FFT) is a method for efficiently computing the DFT of a time series (discrete data samples). The efficiency of this method is such that solutions too many problems can now be obtained substantially more economically than in the past. Thus, the FFT is a highly efficient procedure for computing the DFT of a time series. It takes advantage of the fact that the calculation of the coefficients of the DFT can be carried out iteratively, which results in a considerable savings of computation time. The FFT is a discrete Fourier transform algorithm which reduces the number of computations needed for N points from $2N^2$ to $2N \lg N$, where lg is the base-2 logarithm.

In the present study, the experimental data on the free vibration signal of a rectangular bar specimen made from medium carbon steel S50C were measured for various accelerometer positions using an impulser. The recorded signals were analyzed using Fast Fourier Transform analysis and normalization process has been performed. Finally, the obtained normalization magnitudes were utilized to evaluate the optimal sensor mounting position.

2. Methodology

The type of material for the specimen involved in this study is a medium carbon steel S50C. The specimen is a rectangular bar shape (ASTM, 2015) with the size of 300 × 50 × 10 mm (length × width × thickness) as shown in Fig. 1. To determine the optimal sensor mounting position, type of specimen used in this paper is constrained to be one type of material and one fixed dimension. Material properties of the specimen are given in Table 1.
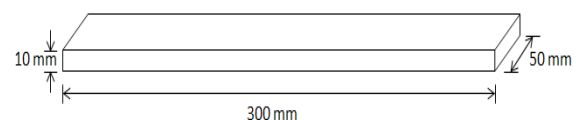

Fig. 1: Specimen for impulsive excitation test

Table 1: Material properties of the specimen

Material	Young's Modulus (GPa)	Poisson's Ratio	Yield Strength (MPa)	Tensile Strength (MPa)	Density (kg/m³)
Medium carbon steel S50C	213.9	0.29	364.8	637.5	7833.4

Impulsive excitation test as shown in Fig. 2 was carried out to investigate the optimal sensor

mounting position. In the experimental set-up, the specimen was placed on the sponge. The

accelerometer was mounted in several positions. An impulser used in this study is a single ball bearing glued to the end of a pencil. The position of the impulsive point is constant along the experiment which is at the center of the specimen.
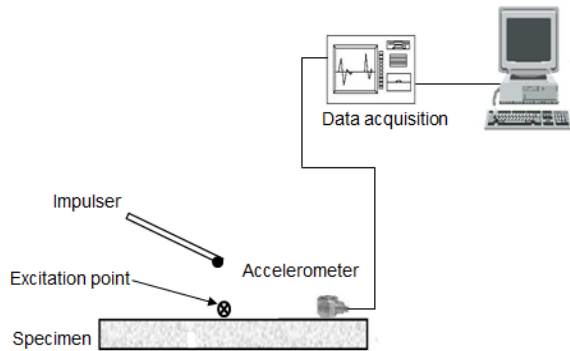

Fig. 2: Experimental set-up

The position of the accelerometer was varied as shown in Fig. 3. These positions were measured from the impulsive point and classified into 6 points which are 4 cm, 6 cm, 8 cm, 10 cm, 12 cm and 14 cm. The specimen was impacted lightly using an impulser at the impulsive point. The impulsive force is mainly hand-controlled by the light impulse. The vibration signal from the specimen was measured using an accelerometer mounted on the first position which is 4 cm from the impulsive point. The impact experiment was repeated for five times to get an average value. Then, same experimental procedures were performed with different accelerometer position.
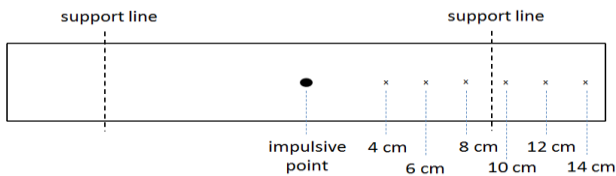

Fig. 3: Sensor mounting position

3. Results and discussion

The specimen was impacted lightly using an impulser at the centre of the specimen. Based on the repeatability between test measures, it is recommended that at least 5 repetitions of the test be performed to reduce any impact point effects. Fig. 4 presents the vibration signal of the dynamic response of the specimen at sensor positions 4 cm, 6 cm, 8 cm, 10 cm, 12 cm and 14 cm respectively. The generated time domain is a transient decaying signal. The vibration level increase drastically after impulsive force and decay to lower the amplitude after the maximum level achieved (Shao and Luo, 2005; Luk et al., 2010). From the observation, these time domain signals show similar characteristic. Unfortunately, no significant differences can be detected between all the time domains. Because the amplitude of the transient vibration signal is meaningless, one cannot evaluate the optimal sensor mounting position. Therefore, the optimal sensor

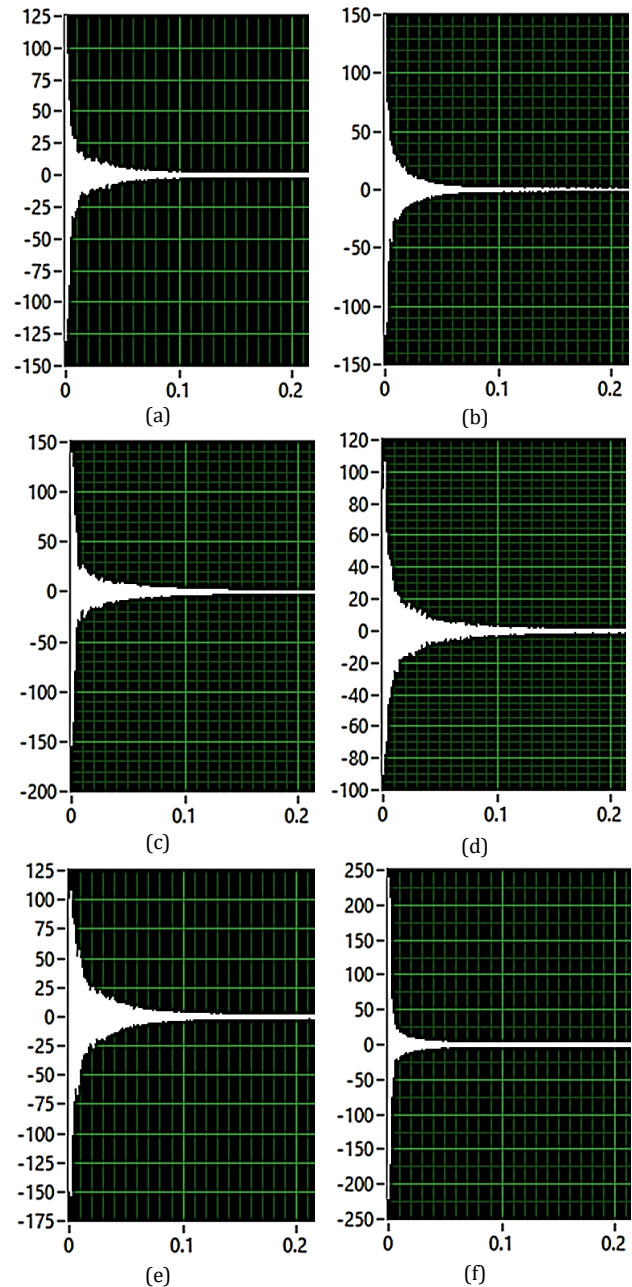mounting position through the time domain is not valid.

Fig. 4: Time domain for sensor position (a) 4 cm (b) 6 cm (c) 8 cm (d) 10 cm (e) 12 cm (f) 14 cm

The main objective of the impulsive excitation test is to obtain the natural frequency information of the system, part or sample (Węglewski et al., 2013; Zhu and Emory, 2005). Accurate values of natural frequencies are important for further analysis. This accuracy level is relied to the position of the contact sensor. For the optimal sensor mounting position analysis, this work uses the frequency domain characteristics. The frequency domain is then used to identify and characterize the influence of sensor mounting position. The time domain vibration signal plot was converted to frequency domain graph using Fast Fourier Transform method to extract the frequency features. Fig. 5 shows the frequency domain plot from the time domain of each vibration signal.
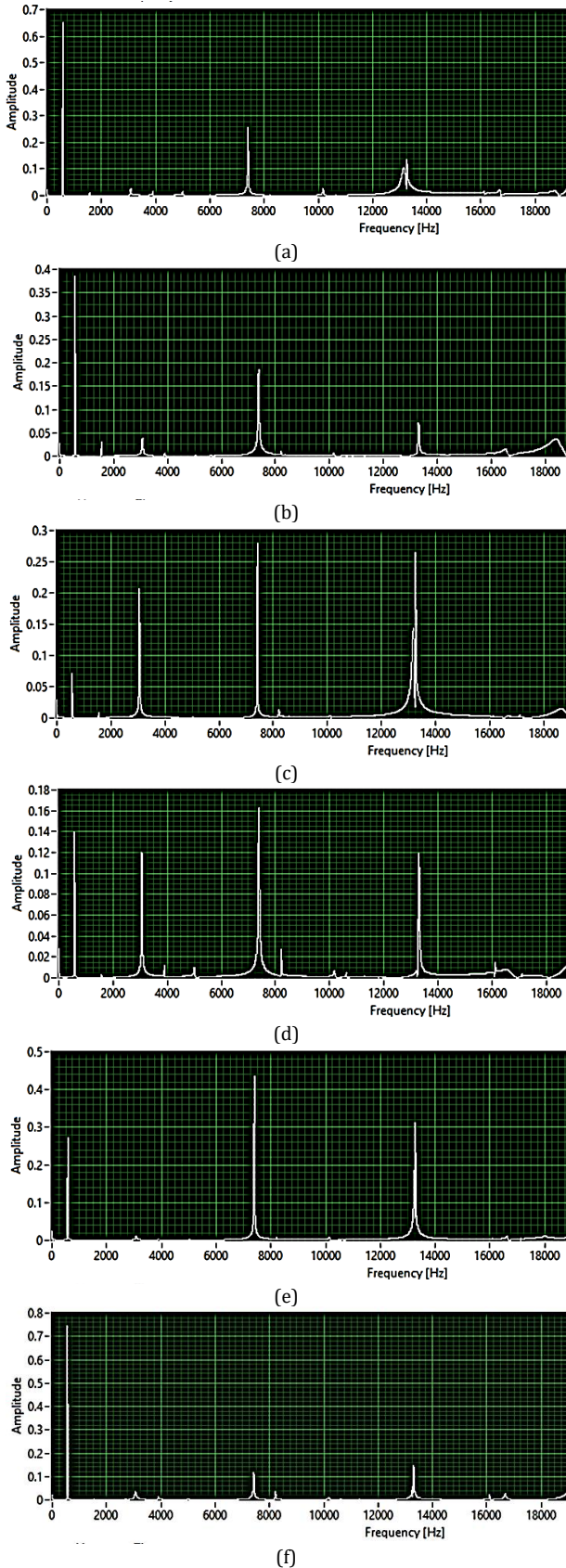
Fig. 5: Frequency domain for sensor position (a) 4 cm (b) 6 cm (c) 8 cm (d) 10 cm (e) 12 cm (f) 14 cm

Frequency domain refers to the natural frequency information of the specimen. As indicated in the figure, it shows that this specimen of medium carbon steel S50C has four natural frequencies. The values are 500 Hz, 3000 Hz, 7500 Hz and 13250 Hz. These values are constant for all sensor mounting positions. Different positions show no influence to the natural frequency values. Since the Fast Fourier Transform will yield several peaks, the magnitude of the peak value for each natural frequency is extracted and reported in Tables 2-7.

Changes in the magnitude of the natural frequency of the transient vibration signal have been analyzed. There is a general agreement between the magnitude of the natural frequency and contact sensor positions.

Table 2: magnitude of the natural frequency values for 4 cm position

Number of Impact	Natural Frequency (Hz)			
	500	3000	7500	13250
a	0.62	0.03	0.26	0.13
b	0.56	0.04	0.26	0.12
c	0.56	0.05	0.23	0.16
d	0.43	0.03	0.16	0.21
e	0.32	0.03	0.17	0.22

Table 3: Magnitude of the natural frequency values for 6 cm position

Number of Impact	Natural Frequency (Hz)			
	500	3000	7500	13250
a	0.35	0.08	0.4	0.07
b	0.35	0.075	0.38	0.05
c	0.34	0.08	0.37	0.05
d	0.35	0.075	0.375	0.05
e	0.35	0.07	0.37	0.04

Table 4: Magnitude of the natural frequency values for 8 cm position

Number of Impact	Natural Frequency (Hz)			
	500	3000	7500	13250
a	0.07	0.21	0.28	0.275
b	0.07	0.21	0.28	0.265
c	0.07	0.21	0.27	0.27
d	0.07	0.20	0.265	0.26
e	0.07	0.22	0.285	0.295

Table 5: Magnitude of the natural frequency values for 10 cm position

Number of Impact	Natural Frequency (Hz)			
	500	3000	7500	13250
a	0.14	0.12	0.16	0.12
b	0.14	0.12	0.17	0.12
c	0.145	0.12	0.17	0.11
d	0.14	0.11	0.17	0.10
e	0.25	0.12	0.17	0.10

Table 6: Magnitude of the natural frequency values for 12 cm position

Number of Impact	Natural Frequency (Hz)			
	500	3000	7500	13250
a	0.28	0.02	0.47	0.32
b	0.28	0.02	0.44	0.31
c	0.28	0.02	0.46	0.30
d	0.48	0.02	0.46	0.32
e	0.49	0.02	0.47	0.32

Table 7: Magnitude of the natural frequency values for 14 cm position

Number of Impact	Natural Frequency (Hz)			
	500	3000	7500	13250
a	0.75	0.05	0.13	0.13
b	0.75	0.05	0.13	0.15
c	0.75	0.04	0.13	0.15
d	0.75	0.05	0.13	0.15
e	0.72	0.04	0.12	0.14

Magnitude characteristic of the natural frequency value has been shown to be highly variable and

sensitive which is associated with sensor position. Therefore, interpretation of the magnitude of the signal is essential. To be able to compare the magnitude in the same natural frequency on different sensor positions, the magnitude of the natural frequency values must be normalized. A magnitude analysis technique known as a normalization process was carried out to the database in order to minimize data redundancy for optimal sensor mounting position determination (Rovšček et al., 2014; Kent, 1983). The maximum value obtained from the frequency domain processed signals during all repetitions of the test is then used as the reference value for normalizing the vibration signal. It refers to the conversion of the magnitude of the signal to a scale relative to a maximum peak level. This post-processing method utilizes natural frequency values from the frequency domain of the recorded signal. Tables 8-13 list the normalize magnitude values of the natural frequency for each position respectively. The results were averaged over all the number of excitations.

Table 8: Normalization magnitude of the natural frequency values for 4 cm position

Number of Impact	Natural Frequency (Hz)			
	500	3000	7500	13250
a	1.00	0.05	0.42	0.21
b	1.00	0.07	0.46	0.21
c	1.00	0.09	0.41	0.29
d	1.00	0.06	0.38	0.49
e	1.00	0.09	0.53	0.69
Average	1.00	0.07	0.44	0.38

Table 9: Normalization magnitude of the natural frequency values for 6 cm position

Number of Impact	Natural Frequency (Hz)			
	500	3000	7500	13250
a	0.88	0.20	1.00	0.18
b	0.92	0.20	1.00	0.13
c	0.92	0.22	1.00	0.14
d	0.93	0.20	1.00	0.13
e	0.95	0.19	1.00	0.11
Average	0.92	0.20	1.00	0.14

Table 10: Normalization magnitude of the natural frequency values for 8 cm position

Number of Impact	Natural Frequency (Hz)			
	500	3000	7500	13250
a	0.25	0.75	1.00	0.98
b	0.25	0.75	1.00	0.95
c	0.26	0.78	1.00	1.00
d	0.26	0.75	1.00	0.98
e	0.24	0.75	0.97	1.00
Average	0.25	0.76	0.99	0.98

Table 11: Normalization magnitude of the natural frequency values for 10 cm position

Number of Impact	Natural Frequency (Hz)			
	500	3000	7500	13250
a	0.86	0.74	1.00	0.74
b	0.82	0.71	1.00	0.68
c	0.85	0.71	1.00	0.65
d	0.85	0.67	1.00	0.61
e	1.00	0.48	0.68	0.40
Average	0.88	0.66	0.94	0.61

From the Tables 8-13, the normalization magnitude is meaningful. For optimal feature selection, the normalize magnitudes were integrated in one dataset to create graphs. As indicated in Fig. 6, all the normalization magnitudes of the 10 cm position for each natural frequency show high values.

Table 12: Normalization magnitude of the natural frequency values for 12 cm position

Number of Impact	Natural Frequency (Hz)			
	500	3000	7500	13250
a	0.60	0.04	1.00	0.68
b	0.64	0.05	1.00	0.70
c	0.61	0.04	1.00	0.65
d	1.00	0.04	0.96	0.67
e	1.00	0.04	0.96	0.65
Average	0.77	0.04	0.98	0.67

Table 13: Normalization magnitude of the natural frequency values for 14 cm position

Number of Impact	Natural Frequency (Hz)			
	500	3000	7500	13250
a	1.00	0.07	0.17	0.17
b	1.00	0.07	0.17	0.20
c	1.00	0.05	0.17	0.20
d	1.00	0.07	0.17	0.20
e	1.00	0.06	0.17	0.19
Average	1.00	0.06	0.17	0.19

It means that when the accelerometer mount at 10 cm position during the impulsive excitation test, the generated magnitude value for all the natural frequencies contribute to high readings. Position 10 cm is near to the support system. This finding indicates that the use of normalization process to identify the optimal contact sensor mounting position for an impulsive excitation test application is valid. The set of test is required in order to ensure maximum accuracy in the data recorded from all positions. In conclusion, the ideal contact sensor position for this study is 10 cm.

4. Conclusion

Impulsive excitation technique is a non-destructive method to determine the elastic properties of materials such as Young's modulus, shear modulus and Poisson's ratio. In this study, we have presented a detailed framework for the investigation of optimal contact sensor mounting position. Specimen used in the experimental work is a rectangular bar made from medium carbon steel S50C and excited by single impulse force using an impulser.

The vibration signal from each single impact performed at the center of the specimen for various different accelerometer positions has been measured. Fast Fourier Transform process has been conducted to obtain the natural frequency information. The magnitudes of the natural frequencies has been normalized and compared for each sensor position. Based on the direct observations from the average normalization results, it can be concluded that the position near to the support system is the optimal contact sensor mounting position.
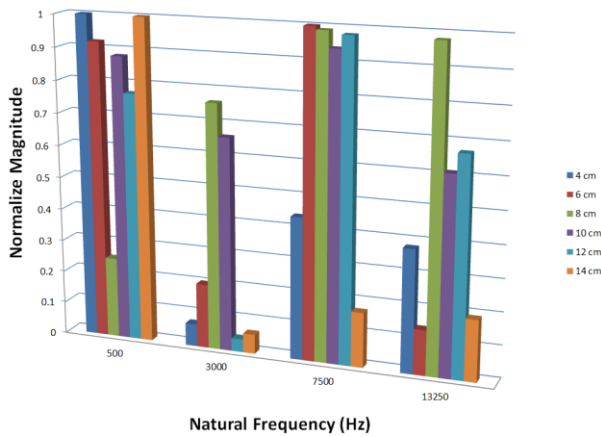
Fig. 6: Comparison of the normalize magnitude

Acknowledgment

References

Abidin HZ, Din NM, Radzi NAM, and Rizman ZI (2017). A review on sensor node placement techniques in wireless sensor networks. International Journal on Advanced Science, Engineering and Information Technology, 7(1): 190-197.

Alfano M and Pagnotta L (2007). A non-destructive technique for the elastic characterization of thin isotropic plates. NDT and E International, 40(2): 112-120.

ASTM (2015). ASTM E1876-15: Standard test method for dynamic Young's modulus, shear modulus, and Poisson's ratio by impulse excitation of vibration. American Society for Testing Materials International, West Conshohocken, USA. Available online at: https://www.astm.org/Standards/E1876.htm

Botelho EC, Campos AN, De Barros E, Pardini LC, and Rezende MC (2006). Damping behavior of continuous fiber/metal composite materials by the free vibration method. Composites Part B: Engineering, 37(2): 255-263.

Groves D and Wachtman J (1985). Materials characterization-vital and often successful, yet still a critical problem. Materials and Society, 9(1): 45-58.

Ito Y and Uomoto T (1997). Nondestructive testing method of concrete using impact acoustics. NDT and E International, 30(4): 217-222.

Kent W (1983). A simple guide to five normal forms in relational database theory. Communications of the ACM, 26(2): 120-125.

Liu SX, Tong F, Luk BL, and Liu KP (2011). Fuzzy pattern recognition of impact acoustic signals for nondestructive evaluation. Sensors and Actuators A: Physical, 167(2): 588-593.

Luk BL, Liu KP, Tong F, and Man KF (2010). Impact-acoustics inspection of tile-wall bonding integrity via wavelet transform and Hidden Markov Models. Journal of Sound and Vibration, 329(10): 1954-1967.

Nyce DS (2004). Linear position sensors: Theory and application. John Wiley and Sons, Hoboken, USA.

Plachy T, Padevet P, and Polak M (2009). Comparison of two experimental techniques for determination of Young's modulus of concrete specimens. In the Conference of Recent Advances in Applied and Theoretical Mechanics, Montreux, Spain: 68-71.

Policarpo H, Neves MM, and Maia NMM (2013). A simple method for the determination of the complex modulus of resilient materials using a longitudinally vibrating three-layer specimen. Journal of Sound and Vibration, 332(2): 246-263.

Prasad DR and Seshu DR (2008). A study on dynamic characteristics of structural materials using modal analysis. Asian Journal of Civil Engineering, 9(2): 141-152.

Radovic M, Curzio EL, and Riester L (2004). Comparison of different experimental techniques for determination of elastic properties of solids. Materials Science and Engineering: A, 368(1): 56-70.

Raggio L, Etcheverry J, and Bonadeo N (2007). Determination of acoustic shear and compressional wave velocities for steel samples by impulse excitation of vibrations. In the Conferencia Panimericana de END, Asociacion Argentina de Ensayos No Destructivos y Estructurales (AAENDE), Buenos Aires, Argentina: 1-9.

Renault A, Jaouen L, and Sgard F (2011). Characterization of elastic parameters of acoustical porous materials from beam bending vibrations. Journal of Sound and Vibration, 330(9): 1950-1963.

Rovšček D, Slavič J, and Boltežar M (2014). Operational mode-shape normalisation with a structural modification for small and light structures. Mechanical Systems and Signal Processing, 42(1): 1-13.

Salem JA and Singh A (2006). Polynomial expressions for estimating elastic constants from the resonance of circular plates. Materials Science and Engineering: A, 422(1): 292-297.

Sanliturk KY and Koruk H (2013). Development and validation of a composite finite element with damping capability. Composite Structures, 97: 136-146.

Santos JPLD, Amaral PM, Diogo AC, and Rosa LG (2013). Comparison of Young's moduli of engineered stones using different test methods. Key Engineering Materials, 548: 220-230.

Shao T and Luo J (2005). Response frequency spectrum analysis for impact behavior assessment of surface materials. Surface and Coatings Technology, 192(2-3): 365-373.

Tognana S, Salgueiro W, Somoza A, and Marzocca A (2010). Measurement of the Young's modulus in particulate epoxy composites using the impulse excitation technique. Materials Science and Engineering: A, 527(18): 4619-4623.

Tong F, Tso SK, and Xu XM (2006). Tile-wall bonding integrity inspection based on time-domain features of impact acoustics. Sensors and Actuators A: Physical, 132(2): 557-566.

Węglewski W, Bochenek K, Basista M, Schubert T, Jehring U, Litniewski J, and Mackiewicz S (2013). Comparative assessment of Young's modulus measurements of metal-ceramic composites using mechanical and non-destructive tests and micro-CT based computational modeling. Computational Materials Science, 77: 19-30.

Zhu WD and Emory BH (2005). On a simple impact test method for accurate measurement of material properties. Journal of Sound and Vibration, 287(3): 637-643.